OPEN ACCESS

The Effect of Chlorides on the Performance of DME/Mg[B(HFIP)$_4$]$_2$ Solutions for Rechargeable Mg Batteries

Journal of The Electrochemical Society, 2023 **170** 090542

The Effect of Chlorides on the Performance of DME/Mg[B(HFIP)$_4$]$_2$ Solutions for Rechargeable Mg Batteries

Ben Dlugatch,[1,z] Janina Drews,[2,3] Ran Attias,[4] Bar Gavriel,[1] Adar Ambar,[1] Timo Danner,[2,3] Arnulf Latz,[2,3,5] and Doron Aurbach[1,*]

[1]*Department of Chemistry, Bar-Ilan University, Ramat Gan 5290002, Israel*
[2]*German Aerospace Center (DLR), Institute of Engineering Thermodynamics, Stuttgart, Germany*
[3]*Helmholtz Institute Ulm for Electrochemical Energy Storage (HIU), Ulm, Germany*
[4]*Space Environment Department, Soreq NRC, Yavne 81800, Israel*
[5]*Institute of Electrochemistry, Ulm University (Ulm), Ulm, Germany*

One of the major issues in developing electrolyte solutions for rechargeable magnesium batteries is understanding the positive effect of chloride anions on Mg deposition-dissolution processes on the anode side, as well as intercalation-deintercalation of Mg^{2+} ions on the cathode side. Our previous results suggested that Cl^- ions are adsorbed on the surface of Mg anodes and Chevrel phase $Mg_xMo_6S_8$ cathodes. This creates a surface add-layer that reduces the activation energy for the interfacial Mg ions transportation and related charge transfer, as well as promotes the transport of Mg^{2+} from the solution phase to the Mg anode surface and into the cathodes' host materials. Here, this work further examines the effect of adding chlorides to the state-of-the-art Mg[B(HFIP)$_4$]$_2$/DME electrolyte solution, specifically focusing on reversible magnesium deposition, as well as the performance of Mg cells with benchmark Chevrel phase cathodes. It was observed that the presence of chlorides in these solutions facilitates both Mg deposition, and Mg^{2+} ions intercalation, whereby this effect is more pronounced as the purity level of the solution is lowered.

 [DOI: 10.1149/1945-7111/acf960]

Manuscript submitted July 31, 2023; revised manuscript received September 10, 2023. Published September 27, 2023.

The future of the renewable, green energy field depends on progress in several key technologies. Some of the more prominently developing technologies are devices for large energy storage. Magnesium-metal anode-based batteries are suitable candidates for this purpose due to the high abundance of Mg in Earth crust, low redox potential and high volumetric and gravimetric capacity, the chance to have non-dendritic deposition processes, low price, and relatively good safety features.[1,2]

On the one hand, the high charge density of the bivalent magnesium cation enables high energy densities. On the other hand, it causes strong coulombic interactions with anions, and solvent molecules, which leads to high energetic barriers for de-solvation, and solid-state diffusion. This can hinder the electrochemical reactions on both electrodes, and strongly limit the performance of any Mg batteries prototypes.[1,3,4]

Most polar-aprotic solvents relevant to active metal (Li, Na) based rechargeable batteries like esters and alkyl carbonates are reactive with Mg metal. Therefore, for rechargeable Mg battery systems, the most relevant solutions are based on ether solvents.[5] Ether solvents are not reactive with metallic Mg electrodes, yet they can effectively dissolve some Mg salts, and form solutions with a reasonable ions separation, forming ionic conductivity. Many ethereal solutions of Mg salts form complex structures, due to strong interactions between Mg ions and the ethereal solvents' oxygen atoms. A classic example includes solutions comprising of Mg salt like $Mg(N(SO_2CF_3)_2)_2$ (MgTFSI) in di-methoxy-ethane (DME) that forms strongly solvated $Mg(DME)_3^{2+}$ complexes (the $TFSI^-$ anions are relatively free in solution), that impede pronouncedly both Mg deposition and Mg^{2+} ions intercalation reactions with these solutions. The presence of chlorides in these solutions (e.g., in MgTFSI/DME/$MgCl_2$ solutions) change their complex structure, and chlorides partially replace the solvent molecules of the first coordination shell, which remarkably softens the de-solvation of Mg ions, thus facilitating both Mg deposition and Mg ions intercalation reactions in these solutions.[6,7]

Therefore, most of the electrolyte solutions that support reversible Mg deposition reported so far contain chlorides.[5] Chlorides may play two roles in ethereal Mg salt solutions. Focusing on DME solutions as an important example, the chlorides interact with magnesium cations, forming $MgCl^+$ or $Mg_2Cl_3^+$ complexes surrounded by DME molecules.[7] These complexes weaken the interactions between Mg ions and their solvation shells which reduces the de-solvation energy of Mg^{2+} ions.[6,8] In addition, it was suggested that chloride ions in solutions may form add-layers on the anode and cathodes surface that decreases the activation energy of Mg ions transfer from the solution phase to the solid structure of the electrodes.[9]

However, chlorides can negatively promote corrosion of the metallic current collectors of the cathodes, usually thin aluminum foils.[10]

To avoid those issues a lot of recent research has also focused on chloride-free electrolyte systems for Mg batteries.[11] Thereby, the most promising solution that is capable of reversible Mg deposition at room temperature was found to be magnesium tetrakis(hexafluoroisopropyloxy)borate (Mg[B(HFIP)$_4$]$_2$) in dimethoxyethane (DME) solution.[12] Yet, a special pre-treatment is required in order to bring these solutions to any practical importance.[13] The need for such a compulsory pre-treatment is because non-aqueous electrolyte solutions may be contaminated with reactive atmospheric moieties like trace water, oxygen, or trace protic moieties resulting from the electrolyte's synthesis, all of which are reactive with Mg metal. Contaminated electrolyte solutions undergo side reactions with the reactive Mg anodes, which form surface species that passivate the electrodes and blocks intercalation. The pre-treatment required removes the contaminants from the solutions and enables Mg ions to interact with bare, un-passivated electrodes' surfaces. We have termed this pre-treatment as "conditioning" process, which brings the electrolyte solutions to working conditions with Mg metal anodes. The conditioning process can be chemical, namely, adding a reactive species like Grignard reagents that react with all active atmospheric moieties and protic contaminants in solution phase, removes them and thus their detrimental side reactions with the electrodes can be fully avoided. We can also apply electrochemical conditioning pre-treatment by cycling symmetric cells containing Mg metal electrodes with the required electrolyte solution. Repeated

*Electrochemical Society Fellow.
[z]E-mail: bendlugatch@gmail.com

Table I. Basic geometric, transport and kinetic parameters of electrolyte, Mg anode and CP cathode for the simulations.

Parameter	Value
Electrolyte	
Distance between the electrodes	1 cm
Conductivity κ for 0.3 M $Mg[B(HFIP)_4]_2$/DME	1.1 S m^{-1}
Conductivity κ for 0.3 M $Mg[B(HFIP)_4]_2$ + 0.6 M $MgCl_2$/DME	2 S m^{-1}
Diffusion coefficient D_e	10^{-10} m^2 s^{-1}
Transference number t_+	0.21
Anode	
Butler-Volmer rate constant k_{BV}	$5.1 \cdot 10^{-9}$ m s^{-1}
Symmetry factor α_{BV}	0.359
Cathode	
Mo_6S_8	80 wt%
Carbon Black	10 wt%
PVDF	10 wt%
Porosity ϵ_s	0.52
Bruggeman coefficient β	3.45
Maximum Mg concentration per site c_{max}	5722 mol m^{-3}

cycling exposes the solution to fresh Mg deposits that react with all the contaminants and remove them from the solution phase. Applying such electrochemical conditioning processes to ($Mg[B(HFIP)_4]_2$)/DME solutions significantly improve their electrochemical performance, albeit the coulombic efficiency of reversible Mg deposition processes with them during the first cycles (around 95%) is relatively low.[13]

Until now, the Chevrel-phase $Mg_xMo_6S_8$ ($0< \times <2$) is the benchmark cathode material for rechargeable magnesium batteries due to its high Mg^{2+} ions intercalation-deintercalation reversibility, even though the maximal specific capacity is only around 120 mAh g^{-1}, and the average discharge voltage is low at around 1.1 V.[14] The field of Mg batteries in very vital in recent years, with literature including many papers reporting on extensive experimental studies[15] and DFT calculations.[16,17] There are also very recent reports on modeling approaches on continuum scales to get more insights into undesired limitations and to provide design strategies for optimizing the performance of Mg batteries prototypes.[18] Although the Chevrel Phase (CP) cathodes were mostly studied in chloride-containing electrolyte solutions for Mg batteries, it has already been shown that reversible magnesium intercalation is also possible from the Cl−free $Mg[B(HFIP)_4]_2$/DME electrolyte solutions.[18,19] However, Mg ions' insertion and de-insertion processes with CP cathodes in these important solutions were not explored enough to enable reaching progress toward practical applications. The necessary scientific insights here have not reached yet.

The aim of this work was to provide more insights into the effect of chlorides on the performance of state-of-the-art electrolyte solutions for rechargeable magnesium batteries. Therefore, we systematically study the effect of adding chlorides (in the form of $MgCl_2$) to $Mg[B(HFIP)_4]_2$/DME solutions on Mg deposition-dissolution in conditioned and unconditioned electrolyte solutions, as well as on the performance of full cells comprising of Chevrel-phase cathodes and magnesium metal foil anodes. The experimental results are supported by a detailed analysis of the intercalations kinetics in the different electrolyte solutions based on continuum simulations.

Methodology

$Mg[B(HFIP)_4]_2$ synthesis and chemical characterization.—All experiments were done in an argon-filled glove box (H_2O and O_2 < 0.1 ppm).

$Mg[B(HFIP)_4]_2$ was synthesized as described in a previous work.[20] The Cl−free electrolyte solutions were prepared by adding $Mg[B(HFIP)_4]_2$ into DME to reach 0.3 M and stirred for 12 h. The solutions containing chlorides were similarly prepared by adding $Mg[B(HFIP)_4]_2$ into DME to reach 0.3 M, then additionally adding $MgCl_2$ to reach the desired Cl− anions concentrations (0.6, 0.3, 0.1, and 0.05 M). After adding the two magnesium salts into DME, the solutions were stirred for 24 h at 35 °C.

Chevrel phase (CP) was synthesized following a procedure described in a past work.[3] The CP composite electrodes were prepared by mixing CP with PVDF, and carbon-black in weight percentage of 80%, 10%, and 10% respectively. The slurry was used to coat 1 × 1 cm^2 Pt current collectors, then dried on a hot plate for 2 h before entering the glovebox. The mass-loads of the cathode materials were calculated by the weight differences before and after coating.

Herein, we use CP electrodes that are termed "activated CP cathodes." This entails cycling CP electrodes in 0.3 M $Mg[B(HFIP)_4]_2$/0.6 M $MgCl_2$/DME solutions for 5 cycles at 0.05 mV s^{-1} vs Mg metal foil counter electrodes. Afterwards the electrodes were washed with DME and transferred into the chloride-free electrolyte solutions.

Electrochemical characterizations.—Electrochemical characterizations of the electrolyte solutions were carried using mechanically scraped Mg foils as counter electrodes (CE) and reference electrodes (RE), For cyclic voltammetry (CV), 0.5 mm diameter Pt wires were used as working electrodes (WE), while for galvanostatic experiments, 1 × 1 cm^2 Pt electrodes were employed as the WE. in three electrodes flooded cells. For the characterization of magnesium intercalation, a similar setup was used with Chevrel Phase coated Pt as WE.

Macro cycling efficiency measurements were carried by the same procedure as described in previous work.[13]

Electrochemical conditioning processes were performed by applying constant 1 mA cm^{-2} current repeatedly for 150 cycles, −1 V, and 2.8 V were set to be the negative and positive cut-off potentials, respectively, in a three electrodes' cells with Pt-mesh WE, and Mg strips as CE & RE.

Continuum modelling.—Recently, a new continuum model was developed, which can describe the complex intercalation process of magnesium into a Chevrel Phase (CP) cathode and a detailed derivation and description of this simulation framework including all relevant equations can be found in previous work.[18] In summary, the model is based on a thermodynamically consistent transport theory,[21] and explicitly considers the unique crystal structure of the CP, which provides two possible sites with different thermodynamics and kinetics for magnesium intercalation and their interplay. The used subscript 1 refers to a parameter of the inner intercalation sites, which are energetically favorable, whereas the subscript 2

indicates that the corresponding parameter belongs to the outer intercalation sites. The kinetics of each of the two intercalation reactions are described by the common Butler-Volmer equation. Moreover, the overall solid-state transport of magnesium in CP is described by contributions of hopping between energetically similar sites (1 ⇌ 1 and 2 ⇌ 2)—which represents classical solid-state diffusion - and jumping from one type of intercalation site to the other (1 ⇌ 2), which is called exchange reaction.

All simulations were performed in MATLAB, whereby the system of conservation equations is numerically solved based on a spatially discretization with the finite-volume method.

The basic parameterization of the model regarding the transport properties of the electrolytes and the electron-transfer kinetics at the magnesium metal anode is transferred from earlier work based on DFT calculations and experimental data and can be found in Table I.[18,22,23]

The additional kinetic and transport parameters for intercalation into untreated and pretreated Chevrel Phase from different electrolytes, which are the solid-state diffusion coefficients for the two intercalation sites D_1 and D_2, the exchange rate constant $k_{2\rightarrow1}$, the Butler-Volmer rate constant for intercalation into the individual sites $k_{BV,1}$ and $k_{BV,2}$ as well as the corresponding symmetry factors $\alpha_{BV,1}$ and $\alpha_{BV,2}$, are determined by a least-square fit to the measured galvanostatic discharge and charge curves. Thereby, the square of the voltage difference as well as the square of the difference between the maximum capacity at the end of the galvanostatic (dis)charge are minimized by the fitting algorithm.

The particle size of the Chevrel Phase is also determined as part of the optimization procedure, whereby consistent values for the particle size r_{CP}, the solid-state diffusion constants D_1 and D_2 as well as the exchange rate constant $k_{2\rightarrow1}$ are used as indicator for a successful parameter optimization.

Results and Discussion

Characterization of $Mg[B(HFIP)_4]_2/MgCl_2$/DME electrolyte solutions for reversible Mg deposition processes.—The full electrochemical characterization of $Mg[B(HFIP)_4]_2$/DME electrolyte solutions, and the effect of electrochemical conditioning were already presented previously.[13] To study the effect of adding chlorides into $Mg[B(HFIP)_4]_2$/DME electrolyte solutions, Mg deposition/dissolution reversibility, overpotential for deposition/dissolution, and Mg deposition morphology were investigated via cyclic voltammetry (CV), chronopotentiometry (CP), and E-SEM measurements.

Figure 1 shows the fifth CV cycle of Mg deposition-dissolution on Pt electrodes in $Mg[B(HFIP)_4]_2$/DME (red line) compared to a similar process in $Mg[B(HFIP)_4]_2/MgCl_2$/DME (blue line) at a scan rate of 50 mV s^{-1}. Figure 1a presents the CVs related to Mg deposition/dissolution processes in as-is, un-conditioned solutions, while Fig. 1b shows the same processes in solutions that underwent electrochemical conditioning processes. It can be seen in Fig. 1a, that a large over-potential is required for deposition in unconditioned Cl-containing solutions (0.7 V vs Mg/Mg2+), and even larger over-potential is needed in unconditioned, chlorides free solutions (0.8 V vs Mg/Mg^{2+}). A large overpotential indicates a poor reversibility of Mg deposition in the unconditioned solutions.[24] In addition, the meaning of lower over-potential is lower energy needed for Mg deposition-dissolution, due to surface layer formed by the chlorides in the solutions, reducing the activation energy.[9,25]

A major difference is seen with conditioned solutions. The Cl-free solutions over-potential, for Mg deposition, decreased to −0.5 V vs Mg/Mg^{2+}, while the over-potential of the $Mg[B(HFIP)_4]_2/MgCl_2$ solution was −0.4 V vs Mg/Mg^{2+}.

In previous work, it was found that in DME/$MgTFSI_2$ based solutions the Mg^{2+} ions have solvation shells of 3 DME molecules, which form strong complexes with high de-solvation energy. With the presence of Cl^- anions, softer complexes of $[Mg_2Cl_3]^+$ and $[Mg_3Cl_4]^{2+}$ are formed, which have weaker interactions with solvating DME molecules, thus exhibiting lower de-solvation energy. This explains sufficiently the lower over-potential for Mg deposition in the chlorides containing solutions.[6,7,26] It is known that DME/$MgTFSI_2$ moieties have a reasonable ion separation in DME solutions, for instance reflected by ionic conductivities suitable for practical use.[12,23]

On the contrary to DME/$MgTFSI_2$, in $Mg[B(HFIP)_4]_2$/DME magnesium can be reversibly deposited, and Mg^{2+} ions can be reversibly intercalated into CP cathodes. This difference can be explained by the fact that $MgTFSI_2$ is more prone to ion-pairing than $Mg[B(HFIP)_4]_2$.[12,23,27,28] Previous work showed that bulky anions decompose much more easily on the Mg anode when they are bound to Mg^{2+}.[29] While ion pairs in $MgTFSI_2$ were already found at practical concentrations,[29] aggregation in $Mg[B(HFIP)_4]_2$ could only be observed close to the solubility limit.[12,20] Moreover, it seems that undesired side reactions are more pronounced with $MgTFSI_2$ solutions. In $MgTFSI_2$/DME solutions, decomposition of the anion might form a passivation layer on the Mg surface.[29–31] The anodes' surface in $Mg[B(HFIP)_4]_2$/DME solutions stays passivation-free and enables sufficiently fast Mg deposition.[29–31] Interestingly, when the DME/$MgTFSI_2$ solutions contain Cl^- anions (e.g., by adding $MgCl_2$) the presence of chlorides moieties changes the $MgDME_3^{2+}$ cations structure and facilitates reversible Mg deposition. One of the reasons may be adsorption of chloride moieties on the Mg surface, which interferes with an easy reduction of TFSI anions, thus mitigating Mg surface passivation and facilitating

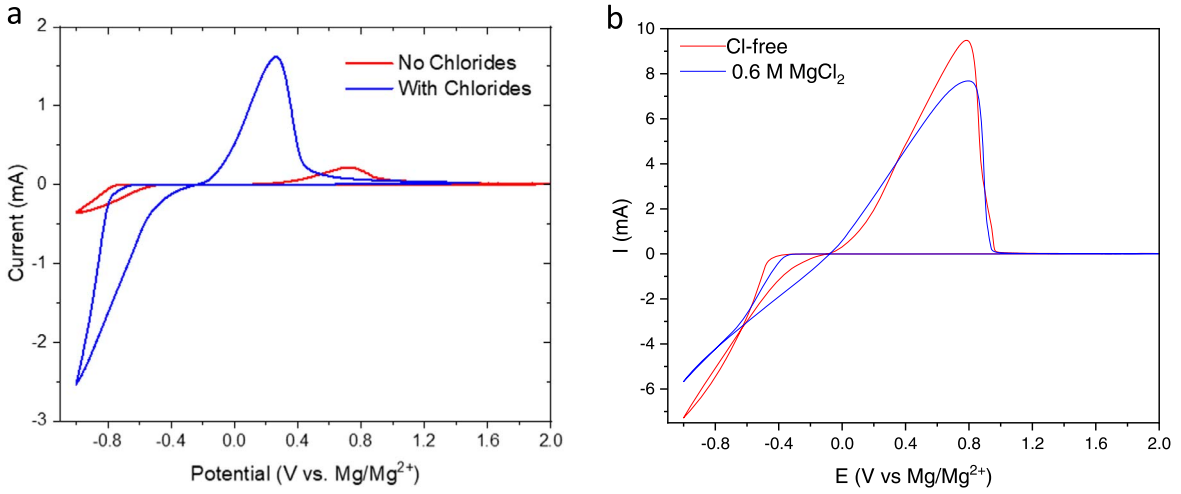

Figure 1. Comparison of the fifth CV cycle with Pt WE in chloride-free and chloride-containing DME/$Mg[B(HFIP)_4]_2$ solutions (a) before, and (b) after conditioning. Mg foils were used as RE and CE, at 50 mV s^{-1} within the potential range −1 and 2 V vs Mg/Mg^{2+}.

Table II. Calculated columbic efficiencies (micro cycling efficiency) from CVs [at 50 mV s^{-1}] in $Mg[B(HFIP)_4]_2$/DME solutions with and without chlorides.

	With Chlorides	No Chlorides
Before conditioning	60%	74%
After conditioning	97.9%	95.7%

reversible Mg deposition. The unique structure of $Mg[B(HFIP)_4]_2$ in DME solutions and the lower reactivity of the anions towards reduction on the Mg metal surfaces, enable reversible Mg deposition without the need of additives in solutions.

As clearly seen in Fig. 1, the effect of the chlorides in unconditioned solutions is very pronounced, while after conditioning (i.e., in purified solutions) the effect of the chlorides is rather minor. Moreover, the current densities of the Mg deposition/dissolution processes with the chloride-free pre-treated (conditioned) solutions are higher, compared with chloride containing pre-treated electrolyte solutions, but it can be caused by the different length of Pt wire (WE) dipped in the solutions. However, the Mg-deposition over-potential is lower with chlorides. Adsorption of chlorides layer on the electrodes surface may on the one hand, improves thermodynamic processes by facilitate the ions transfer from the solution to the electrode, and vice versa.[9,25] On the other hand, the adsorption layer may lower the kinetics of Mg deposition/dissolution processes, because the Mg ions transport has to include migration through an adsorbed chlorides layer.

Another thing to conclude from Fig. 1b is that Mg deposition occurs with a different mechanism. In the Cl-free solutions, the loop at the end of the reduction process indicates a classical nucleation, and growth mechanism. While in the solutions containing chlorides, this loop isn't observed, indicating that chlorides are involved in Mg deposition and significantly impact required energetic barriers, which leads to a different reaction mechanism.

Table II presents the columbic efficiencies (in voltametric measurements, what is termed micro cycling efficiency) of Mg deposition/dissolution in both solutions, based on the results related to Fig. 1. Since the untreated solutions exhibit poor deposition-dissolution of Mg, cycling efficiency measurements with them are not important. As presented in Table II, with pre-treated (conditioned) solutions, the presence of chlorides presents a positive effect on the columbic efficiency of the magnesium deposition-dissolution process. This result is coherent with the above explanation about the positive chlorides effect on Mg surfaces passivation mitigation. The presence of chlorides must also have a bulk effect—weakening the interactions between the Mg cations and the DME molecules, thus facilitating Mg ions transport from solution phase to the electrodes' surfaces.

Interestingly, after conditioning the Cl-free solution turned into black suspension,[6,13] while the Cl^- anions containing solution remained clear with a black precipitate at the bottom of the cell. These noticeable differences between the two solutions remained during all the following electrochemical measurements, after the solutions were stored in the glove box for a long period of time as well. As mentioned above, the difference in colors must mean that the presence of chlorides has both bulk and surface effects. The strong impact of chlorides on Mg deposition in unconditioned solutions can be explained by surface effects. Adsorption of chlorides on the electrode's surface may inhibit side reactions with contaminants which are pronounced with untreated solutions, thus enabling better interactions of the polarized electrodes with Mg ions.

In order to test the Mg deposition morphology differences between Cl−free, and Cl−containing electrolyte solutions, we used E-SEM. Figure 2 presents the Mg deposition morphology differences between Cl-free, and Cl-containing electrolyte solutions. It seems that the Mg crystals deposit from the Cl^- anions containing solution are smaller in size and have sharper shape than the crystals deposit from the chloride-free solution. Still, in both the samples we could see decent coverage of the Pt surface by Mg crystals.

To optimizes the chloride concentration, Mg deposition experiments were carried using conditioned solutions with different $MgCl_2$ concentrations. Figure 3 presents cyclic voltammograms of $Mg[B(HFIP)_4]_2$/DME electrolyte solutions without chlorides, and with 0.05 M, 0.1 M, 0.3 M, and 0.6 M of $MgCl_2$ containing solutions, showing the response of Mg deposition/dissolution processes, at a scan rate of 50 mV s^{-1}. The chloride free solution has the highest over-potential for magnesium deposition. It seems that solutions containing 0.3 M $MgCl_2$ solution has a preferred performance, considering the relatively high current densities and lowest overpotential for Mg deposition/dissolution processes, meaning the lowest de-solvation energy, and higher Mg deposition/dissolution kinetics.

Since coulombic efficiency is an important parameter based on the voltammograms in Fig. 3, micro-cycling efficiencies were calculated. Table III presents the difference in coulombic efficiency between the five Cl concentrations. 0.6 M $MgCl_2$ perform the highest efficiency, therefore we continue our work on full cells with this concentration.

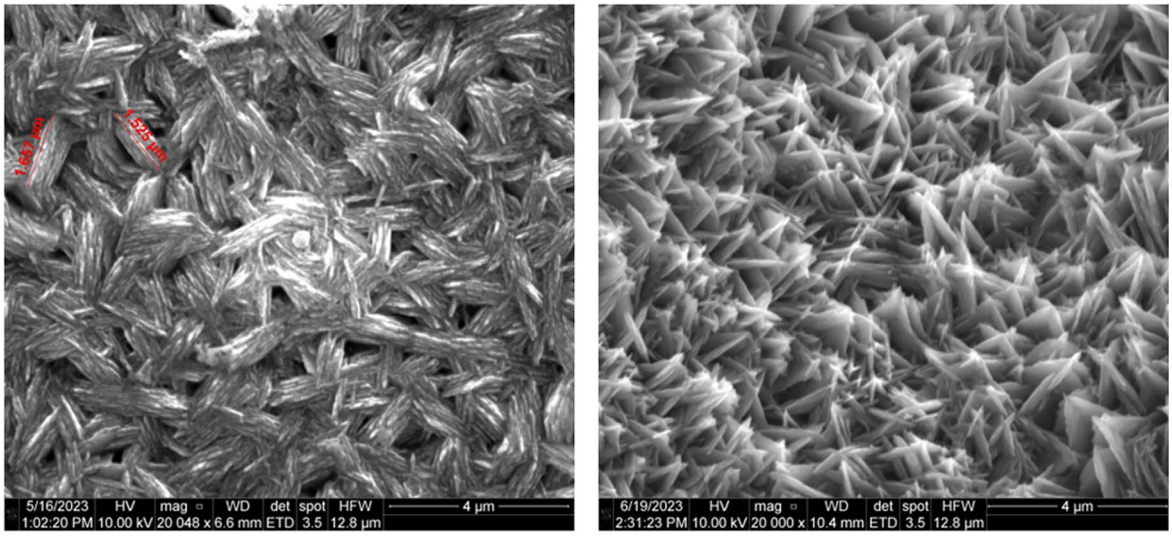

Figure 2. E-SEM images magnesium deposition at 1 mA cm^{-2} for 42 min from $Mg[B(HFIP)_4]_2$/DME (left), and $Mg[B(HFIP)_4]_2/MgCl_2$/DME (right) electrolyte solutions.

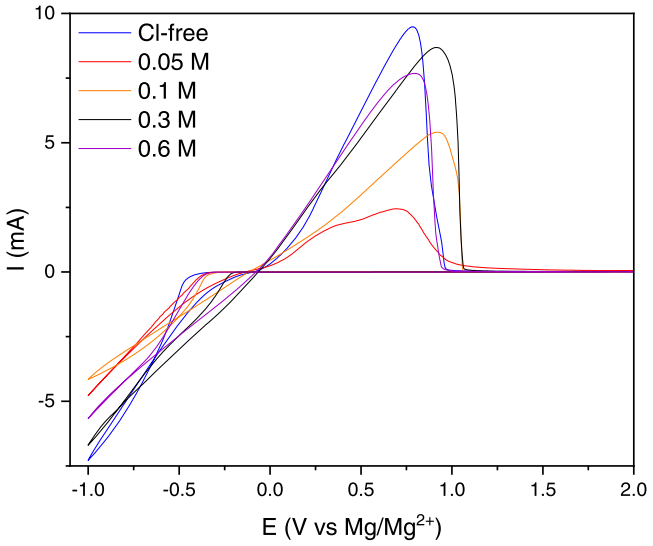

Figure 3. Cyclic voltammograms of Cl−free, 0.05 M, 0.1 M, 0.3 M, and 0.6 M $MgCl_2$ containing DME/$Mg[B(HFIP)_4]_2$ solutions, showing the response of Mg deposition/dissolution processes at a scan rate of 50 mV s^{-1}, using Pt rod as WE, and Mg foil as CE, and RE.

Table III. Coulombic efficiencies (micro-cycle efficiency) of Mg[B (HFIP)4]2/MgCl2/DME with different chlorides concentrations.

Cl concentration (M)	Cl-free	0.1	0.1	0.3	0.6
efficiency	95.7	57.6	94.0	93.1	97.9

To test the $Mg[B(HFIP)_4]_2/MgCl_2$/DME solutions' electrochemical window, CV experiments were run in the range of −1 to 4 V vs Mg/Mg^{2+} (Fig. 4). The electrochemical window of the unconditioned solutions is 3.2 V vs Mg/Mg^{2+}. By conditioning the solutions, the electrochemical window of the solutions was extended to 3.42 V vs Mg/Mg^{2+}. The presence of chloride ions in solutions doesn't affects the electrochemical windows, thus, an electrochemical window of 3.4 V vs Mg/Mg^{2+} is close to the DME's electrochemical window, reflecting well the typically expected anodic stability of ether solvents.[26]

Platinum foils (as used for the above basic experiments) cannot be considered as current collectors in practical systems. For the cathode (positive) side, the choice of current collectors with high enough anodic stability is critically important. The options for Mg batteries may be stainless steel or aluminum. Figure 5 shows the anodic stability of aluminum and stainless-steel in DME/$Mg[B(HFIP)_4]_2$ and DME/$Mg[B(HFIP)_4]_2/MgCl_2$ solutions. Interestingly, the anodic stability with stainless steel (SS) is better than with Al. It seems that SS develops passivation in the chlorides containing solutions, an interesting phenomenon that deserves further studies. Additionally, the anodic stability of the chloride's free solutions (electrodes + solutions) seems to be higher. It is possible that the lack of chlorides forms more stable and strong Mg complexes with the solvent that increase the anodic stability. More experiments are needed to fully understand the anodic behavior of these solutions and possible passivation phenomena related to them. Other options may be $Cl_{2(g)}$ evolution in the solutions containing chlorides, and Al dissolution, catalyzed by the presence of Cl anions that weakens the native passivation of aluminum. A detailed study related to optimal current collectors and a comprehensive understanding of the anodic stability of the above-described systems is beyond the scope of the work presented herein.

To test the true electrochemical behavior and reversibility of these electrolyte solutions, constant current charge-discharge measurements were performed. We term them Macro-cycling efficiency tests. In these experiments, Mg is deposited on Pt initially at

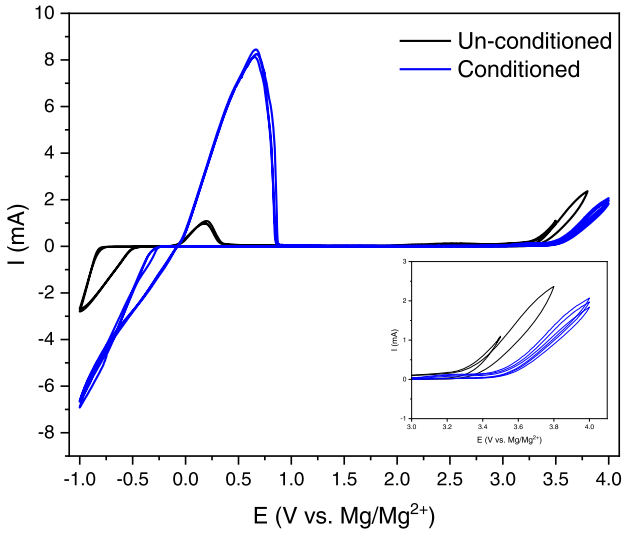

Figure 4. Electrochemical window of Un-conditioned (black line), and Conditioned (blue line) 0.3 M $Mg[B(HFIP)_4]_2$/0.6 M $MgCl_2$/DME solutions, at a scan rate of 50 mV s^{-1}, using Pt as WE, and Mg foil as RE, and CE.

relatively high areal capacity and then, continuous cycling experiments are being conducted (galvanostatic, constant current) in which only 20% of the Mg deposited is being cycled. The cycling can continue until there is no extra Mg deposits left on the Pt electrodes' surfaces (well expressed by the voltage profiles of the dissolution processes), or after several pre-determined cycles, the residual Mg can be dissolved as the final process. This experiment mimics in the best way the working profile of an active metal anode in rechargeable batteries, thus enabling us to predict the "real" behavior of Mg anodes (in the present case).

Figure 6 presents the potential response of these macro-cycling experiments. In the chlorides free solution (Fig. 6a, we can see an increase in the over-potential during cycling, but the potential doesn't increase to the cut-off potential (2.5 V), meaning that residual deposited Mg remained on the surface for 100 cycles, yielding an average efficiency of 96.3%. Figure 6b shows results of similar experiments with chlorides-containing solutions. With the chloride-containing electrolyte solutions, the electrodes still contained residual Mg deposits during around 87 cycles. At the 87th cycle the potential increased to the cut-off potential, probably meaning that all the magnesium that was deposited at the first step was fully dissolved. Considering these results, the calculated macro cycling efficiency for Mg deposition/dissolution processes in these solutions reached values close to 95.4%. This efficiency is very low for practical systems. However, these experiments exhibit a better performance of the chloride-free solution for rechargeable Mg anodes. In the two systems we can see during these long-term cycling experiments an increase in the over-potential as the cycling experiments proceeded (lower deposition currents, and higher dissolution currents). The conclusion from these experiments is that with DME/$Mg[B(HFIP)_4]_2$ solutions at high enough level of purity, there is no clear positive effect of chlorides in solutions on the reversibility and kinetics of magnesium deposition/dissolution processes, as is similarly the case with non-organometallic ethereal solutions like $MgTFSI_2$/DME. It appears that the intrinsic properties of the DME/$Mg[B(HFIP)_4]_2$, in terms of non-reactivity with Mg metal electrodes and bulk properties that allow a facile interfacial transfer of Mg ions, are sufficiently good and provide a very reasonable basis for a further optimization.

The Effect of the presence of chlorides in solutions on the Mg^{2+} ions intercalation/de-intercalation into chevrel-phase cathodes.— Recent studies of ethereal solutions based on DME and THF solvents revealed that the presence of chlorides in solutions have a

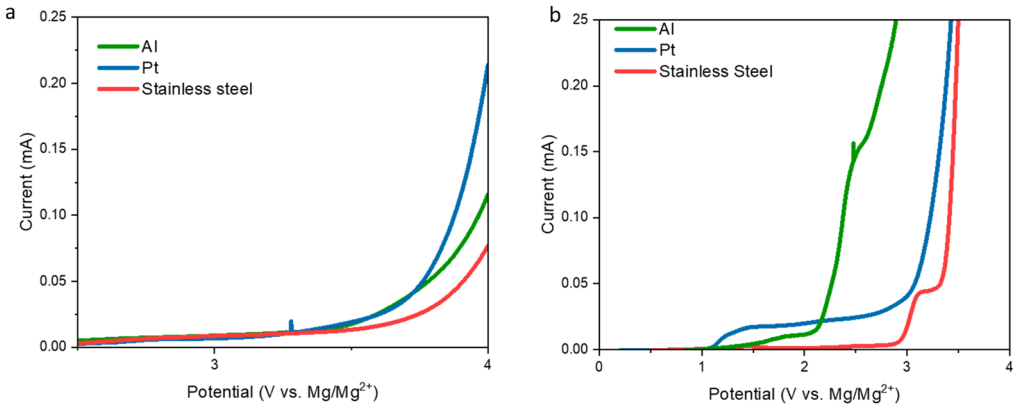

Figure 5. Anodic stability of aluminum and stainless-steel foil electrodes in (a) conditioned 0.3 M $Mg[B(HFIP)_4]_2$/DME, and (b) conditioned 0.3 M $Mg[B(HFIP)_4]_2$/0.6 M $MgCl_2$/DME.

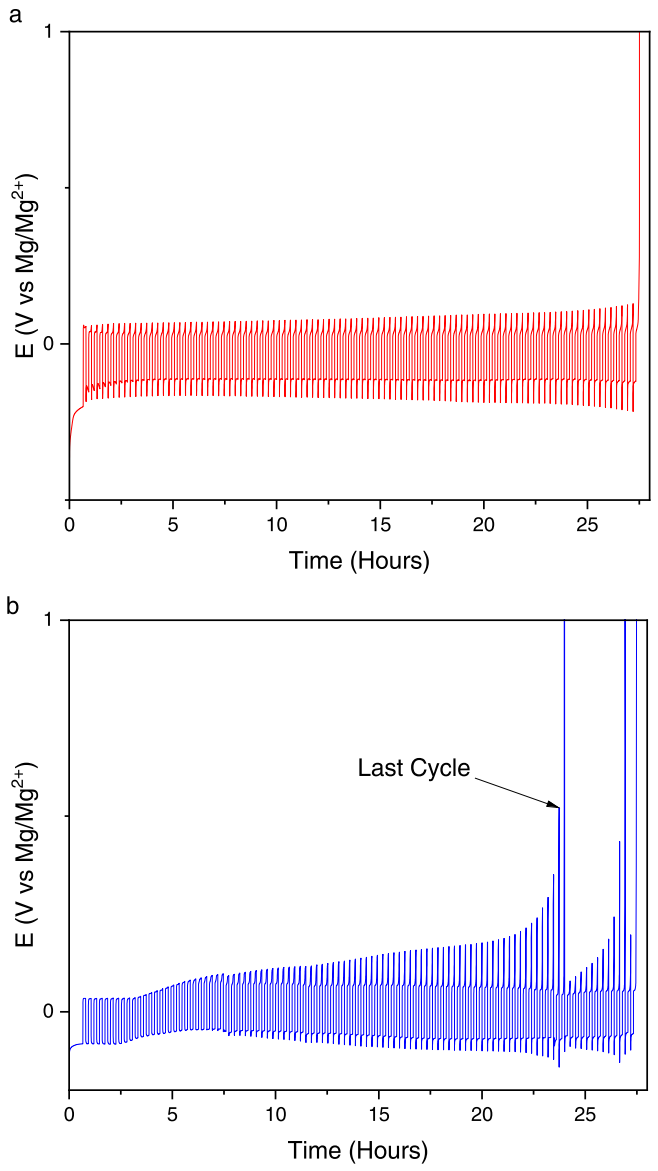

Figure 6. Macro cycling efficiency measurements on a Pt electrode with (a) conditioned 0.3 M $Mg[B(HFIP)_4]_2$/DME (b) conditioned 0.3 M $Mg[B(HFIP)_4]_2$/0.6 M $MgCl_2$/DME electrolyte solutions with Mg as both CE and RE at current density of 1 mA cm^{-2}.

major positive role in allowing insertion of Mg^{2+} ion into Chevrel-phase (CP) cathodes, likely by way of decreasing the activation energy for Mg ions transfer between the solution and the solid structure.[9]

The work described herein presents the comparison between three full-cells systems: (1) CP cathodes, Mg anodes, and 0.3 M $Mg[B(HFIP)_4]_2$/DME electrolyte solution, (2) CP cathodes, Mg anodes, and 0.3 M $Mg[B(HFIP)_4]_2$/0.6 M $MgCl_2$/DME electrolyte solution, and (3) CP cathodes, Mg anodes, and 0.3 M $Mg[B(HFIP)_4]_2$/DME electrolyte solution, but the CP cathodes were cycled before in 0.3 M $Mg[B(HFIP)_4]_2$/0.6 M $MgCl_2$/DME electrolyte solution for 3 cycles, what could create "activated cathodes" due to chloride ions adsorption that remains adsorbed (and may facilitate Mg ions interfacial transport) also after the transfer into the chloride free solutions.[9]

It is important to note that CP cathodes can insert 2 Mg ions per Mo_6S_8 unit, which occupy two types of sites (inner and outer sites) in reversible processes, which are classified as first order phase transition processes. The Mg ions intercalation processes are reflected by two plateaus at around 1.25–1.3 V and 1.1 V vs Mg^{2+}/Mg in galvanostatic processes, or two sets of peaks around these potentials in cyclic voltametric measurements a total maximal specific capacity of 122 mAh g^{-1}, theoretically around 62 mAh g^{-1} per process). Especially at temperatures around 25 °C and below, the second intercalation process occurring between 1.2 and 1.3 V vs Mg^{2+}/Mg may be sluggish. A capacity lower than the theoretical number around 60 mAh g^{-1} reflects some trapping of Mg ions in the inner sites of the CP material.[3,15] Figure 7 presents the 6th CV cycles of the 3 types of CP cathodes of full cells loaded with unconditioned solutions, at a scan rate of 0.05 mV s^{-1}. The cells with the chlorides free solution perform poorly, showing CVs containing only one pair of broad peaks with a wide potential gap between them. These results don't correlate with the chevrel-phase electrodes' phase transitions.[15] It may indicate that the reactions occurring weren't intercalation/de-intercalation, but a reduction and oxidation of residuals, parasitic reactions. In addition, the very broad cathodic and anodic peaks that these CVs include indicate very clearly poor kinetics. With the unconditioned DME/$Mg[B(HFIP)_4]_2$/$MgCl_2$ solutions we obtain the expected voltammograms of Mg^{2+} ions intercalation/de-intercalation processes related to CP cathodes.[3] There is a pair of two sharp intercalation/de-intercalation peaks around 1 V vs Mg^{2+}/Mg, related to the outer sites of the CP crystals and another pair of broad peaks around 1.2 V that reflect much slower reaction, and lower capacity that resulting from trapping of Mg ions in inner sites, at too low temperatures (even at RT). Hence, the presence of chlorides in unconditioned DME/$Mg[B(HFIP)_4]_2$ solutions provide the usually expected voltametric behavior of CP electrodes in ethereal solutions containing active and available Mg ions. Interestingly, as seen in Fig. 7, the cells

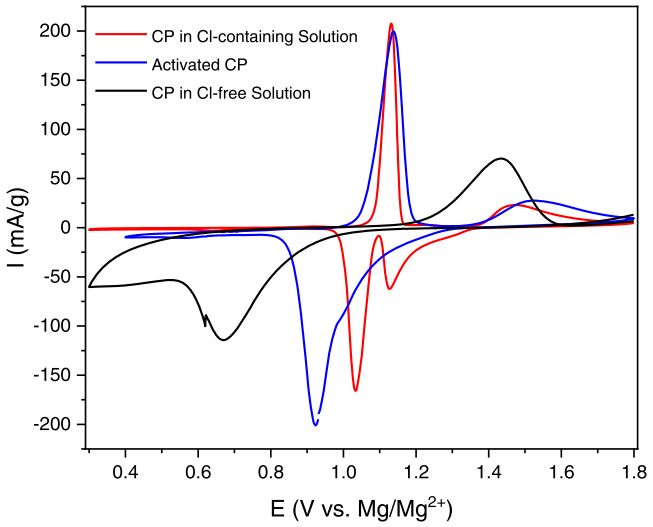

Figure 7. 6th CV cycles at 0.05 mV s^{-1} of CP cathodes in ***unconditioned***/ 0.3 M $Mg[B(HFIP)_4]_2$/DME/Mg anode (black line), Activated CP cathode in ***unconditioned*** 0.3 M $Mg[B(HFIP)_4]_2$/DME/Mg anode (blue line), and in ***unconditioned*** 0.3 M $Mg[B(HFIP)_4]_2$/0.6 M $MgCl_2$/DME (red line).

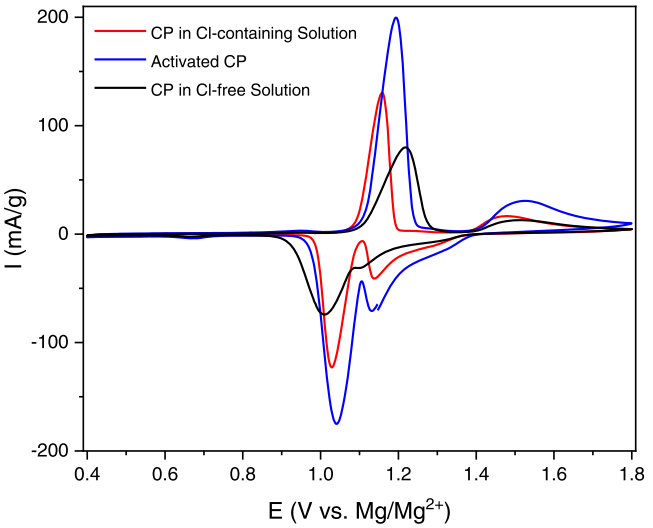

Figure 8. 4th CV cycles at 0.05 mV s^{-1} of CP cathodes in ***conditioned***/ 0.3 M $Mg[B(HFIP)_4]_2$/DME/Mg anode (black line), Activated CP cathode in ***conditioned*** 0.3 M $Mg[B(HFIP)_4]_2$/DME/Mg anode (blue line), and in ***conditioned*** 0.3 M $Mg[B(HFIP)_4]_2$/0.6 M $MgCl_2$/DME (red line).

containing activated CP cathodes in DME/$Mg[B(HFIP)_4]_2$ solutions show a voltametric response that reflects an intermediate performance of the cells containing chlorides, and Cl−free solutions, but much closer to Cl−containing solutions performance, showing the expected positive effect of the chloride species adsorbed on the CP surface, facilitating intercalation of Mg ions into CP electrodes, even in chlorides free solutions.

Altogether, the CV measurements of the cells containing unconditioned solutions indicate that the intercalation processes depend more strongly on the nature of the electrolyte solution, compared to the anodic—deintercalation processes, and the species existing at the CP surfaces upon Mg ions insertion, for which de-solvation may play a crucial role. It can be induced that the lack of chlorides in the solution prevents the creation of Mg-Cl complexes, and thus the de-solvation energy needed to extract the magnesium ions from the solution structures is higher, shown by a bigger potential gap between the peaks, and lower intercalation potentials. We saw very similar behaviors and trends with CP electrodes in $MgTFSI_2$/DME solutions.[9]

Figure 8 shows similar results to those presented in Fig. 7 of voltametric measurements of the 3 types of cells containing the conditioned DME/$Mg[B(HFIP)_4]_2$ solutions, with and without chlorides. Comparing the voltametric responses of the cells presented in Figs. 7 and 8 is striking. First of all, it is important to note that the cells with the conditioned solutions reached their steady state behavior faster than the cells containing the unconditioned solutions (during first 4 cycles compared to 6 cycles, respectively). The conditioning process of the solutions pronouncedly improves the behavior of all 3 types of the cells examined herein, comprising Mg metal anodes and CP cathodes. The representative voltametric responses of the 3 cells become much more similar to each other, compared to the diverse behavior of the cells presented in Fig. 7. The response of the cells with chlorides free DME/$Mg[B(HFIP)_4]_2$ solutions is the worst in terms of current densities, peaks separation, resolution and relatively higher overpotentials (a wider separation between the pairing anodic and cathodic peaks in the two sets of peaks). The voltametric response of the cells with the chlorides containing solutions is the sharpest, reflecting the best resolution and the lowest overpotentials required for all the Mg ions intercalation/deintercalation processes of the CP cathodes. In turn, the cells containing the activated cathodes with chloride-free, pretreated DME/$Mg[B(HFIP)_4]_2$ solutions, showing the highest specific current densities and the highest specific charges of the 4 electrochemical processes that these cells undergo per charge-discharge cycles. Another important finding upon comparing Figs. 7 and 8 is the similarity in the cells responses when the solutions contain chlorides. This means that the effect of conditioning on the performance of CP cathodes in DME/$Mg[B(HFIP)_4]_2$/$MgCl_2$ solutions is rather minor. The results presented herein show important pronounced differences between DME/$Mg[B(HFIP)_4]_2$ solutions and the previously studied DME/$MgTFSI_2$ solutions. With the latter solutions, the presence of chlorides is essential in order to exhibit properly working CP electrodes even with conditioned solutions. With the former solutions, the CP electrodes work reasonably well without the presence of chlorides after a conditioning process. One explanation for this difference might be the formation of a beneficial cathode electrolyte interphase by oxidation of the borate anion when the charge cut-off voltage is chosen sufficiently high. Analogue to adsorbed Mg-Cl complexes, BxOy species at the CP surface seem to facilitate the desolvation of $Mg(DME)_3^{2+}$ and therefore enhance the intercalation kinetics.[32]

Figures 7 and 8 show a decrease in the current density of the intercalation/de-intercalation processes in the Cl-containing solutions while moving from unconditioned to conditioned solutions (red curves). The reason for this phenomenon is yet to be understood, further work needs to be done.

Galvanostatic charge-discharge measurements,at C/10 rate, were conducted and presented in Fig. 9. The graphs related to discharge and charge processes show the expected voltage profiles of Mg ions insertion/de-insertion processes into CP electrodes, which exhibit indeed the two stage (plateaus) behavior. Due to the poor response of cells containing chloride-free, unconditioned DME/$Mg[B(HFIP)_4]_2$ solutions, Fig. 9 does not include their response. The results presented in Fig. 9 are coherent with the CV experiments displayed in Figs. 7 and 8. The unconditioned chloride-containing systems perform much better; however, the measured capacity is quite low as well. It seems that side reactions of contaminants, which might be connected to some kind of surface passivation, strongly limit the reachable capacity of the CP cathodes in unconditioned solutions. However, a significant positive impact of conditioning is observed for all three types of cells. With conditioned solutions, the cells' voltage in both plateaus (see Fig. 9) is much higher during discharge, and lower during charge, indicating better interfacial kinetics. Moreover, the voltage plateaus of the discharge processes of cells containing unconditioned solutions with activated cathodes have noticeably steeper slop than the parallel response of the cells which contain chlorides. This means that an impeding stage of de-solvation

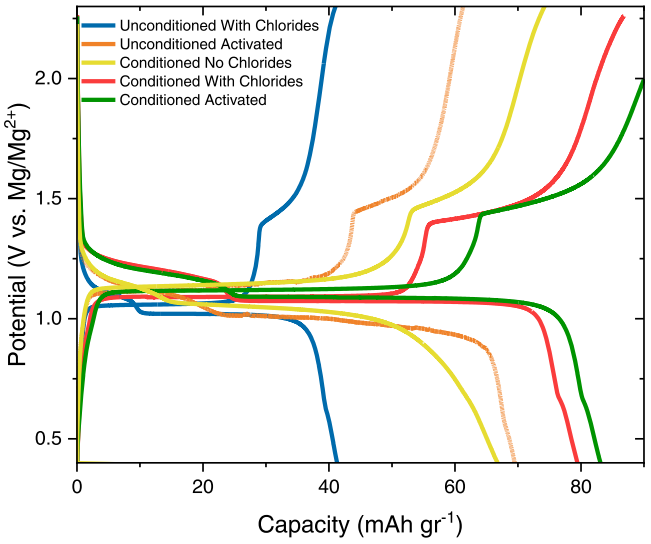

Figure 9. Second cycle charge-discharge curves of chevrel phase electrodes in unconditioned $Mg[B(HFIP)_4]_2/MgCl_2$/DME (blue line), unconditioned $Mg[B(HFIP)_4]_2$/DME after 5 CV cycles in conditioned $Mg[B(HFIP)_4]_2/MgCl_2$/DME (orange line), conditioned $Mg[B(HFIP)_4]_2$/DME (yellow line), conditioned $Mg[B(HFIP)_4]_2/MgCl_2$/DME (red line), and conditioned $Mg[B(HFIP)_4]_2$/DME after 5 CV cycles in conditioned $Mg[B(HFIP)_4]_2/MgCl_2$/DME (green line), when Mg foil was used as CE and RE, at C/10 rates. 0.3 M $Mg[B(HFIP)_4]_2$ in all solutions, and 0.6 M $MgCl_2$ in the relevant solutions.

being required prior to the main charge-transfer processes may play an important role, and significantly impact the kinetics of the overall intercalation reaction. We can conclude that this impeding stage is softened by the presence of chlorides. When the cells containing conditioned solutions, the voltage plateaus that characterize their electrochemical response (in galvanostatic experiments) are much flatter and very similar for the cells containing chlorides, and cells with chlorides free solutions but with activated CP cathodes. For cells with chloride-free conditioned solutions, the plateaus appear at a slightly lower voltage and have a steeper slope, especially for the intercalation into the inner sites of the CP (the first plateau). This behavior implies that de-solvation plays a crucial role and limits the kinetics of the electrochemical reaction, as was already concluded from the CV measurements. However, after a few more galvanostatic cycles the performance of the chloride-free solution improves and the behavior of the discharge-charge curves, especially for the 2nd plateau, gets very similar to the cells with conditioned chloride-containing solutions, showing very stable cycling even after the 2nd cycle. Consequently, it seems that some kind of additional activation process is required for the chloride-free solutions or that the activation requires more time/cycles. This might be connected to the formation of a cathode electrolyte interphase, which is beneficial for the intercalation kinetics.[32] Interestingly, the highest specific capacity is obtained by cells containing activated CP cathodes and chlorides free conditioned solutions. This means that the activation procedure of the CP cathodes (which adds adsorbed chloride moieties to the CP surface) is very effective and implies that the main role of the chlorides is a catalytic effect on the cathode-solution interface, which lowers the energy barrier for the desolvation of Mg ion near the cathodes' surface and therefore facilitates the transfer of the Mg^{2+} from the bulk solution to the Chevrel Phase surface. We emphasize that while a facile intercalation of Mg ions into CP electrodes is possible with conditioned chlorides free $Mg[B(HFIP)_4]_2$/DME solutions, Mg ions insertion into CP electrodes in $MgTFSI_2$/DME requires the presence of chlorides in solutions even after a conditioning process.

Continuum simulations can provide additional insights into the impact of the electrolyte solution on magnesium intercalation into chevrel phase and the experimentally observed differences of the charge-discharge curves. Based on the measured data presented in Fig. 9, the kinetic ($k_{BV,i}$ and $\alpha_{BV,i}$) and transport (D_i and $k_{2\rightarrow1,}$) parameters for magnesium insertion are optimized for each of the electrolyte solutions.

Note that the fitting algorithm was not in all cases able to perfectly minimize the objective function and, especially for the plateaus caused by insertion and extraction into and from the inner sites of the Chevrel Phase. We can still see deviations between measurements and simulations. This indicates that additional processes, like the impact of side reactions from reactive contaminants that are not captured or only indirectly captured in our model, are relevant. However, the results of the parameter optimization are consistent regarding the solid-state transport as well as the CP particle size and also match with findings from previous work (Table I).[18] All optimized parameters from fitting procedure are summarized in Table IV. Moreover, a comparison of the measured and the simulated discharge-charge curves are shown in Fig. 10.

Similar diffusion coefficients D_1, D_2 and exchange rate constants $k_{2\rightarrow1}$ were found for all conditioned electrolyte solutions, which shows that the solid-state transport in the Chevrel Phase particles is independent of the electroactive species. Consequently, the same species seem to intercalate into the host, which implies that co-intercalation of chlorides doesn't play a role and bare magnesium ions are intercalating into the Chevrel Phase.

Interestingly, significantly lower values for the transport parameters are found for the unconditioned electrolyte solutions (Table IV). However, it is very unlikely that the intercalating species changes by conditioning. It rather seems that side reactions of

Table IV. Optimized geometric, kinetic and transport parameters for intercalation into Chevrel Phase from different electrolytes. The highest values for all parameters are highlighted in green, slightly smaller values are marked in yellow and significantly smaller values in red. The corresponding comparison of the simulated and measured charge-discharge curves can be found in Fig. 10.

Electrolyte		D_1 $m^2\ s^{-1}$	D_2 $m^2\ s^{-1}$	$k_{2\rightarrow1}$ $m^3\ s^{-1}\ mol^{-1}$	$k_{BV,1}$ $m\ s^{-1}$	$k_{BV,2}$ $m\ s^{-1}$	$\alpha_{BV,1}$	$\alpha_{BV,2}$	r_{BV} μm
unconditioned	with chlorides	8.0e-19	3.9e-16	6.0e-8	3.3e-9	6.6e-8	0.32	0.17	0.53
	activated	5.1e-19	1.1e-16	5.3e-8	4.3e-9	4.0e-8	0.39	0.16	0.57
conditioned	no chlorides	8.1e-19	1.7e-15	4.3e-7	4.4e-8	8.2e-8	0.12	0.18	0.55
	with chlorides	8.7e-19	1.8e-15	4.6e-7	6.7e-8	1.1e-7	0.35	0.28	0.44
	activated	8.8e-19	1.6e-15	4.4e-7	6.7e-8	9.9e-8	0.34	0.29	0.40
0.3 M $Mg(B[HFIP)_4)_2$ from previous work[18]		7.0e-19	1.9e-15	4.1e-7	4.8e-8	8.1e-8	0.11	0.34	1.26-9.75

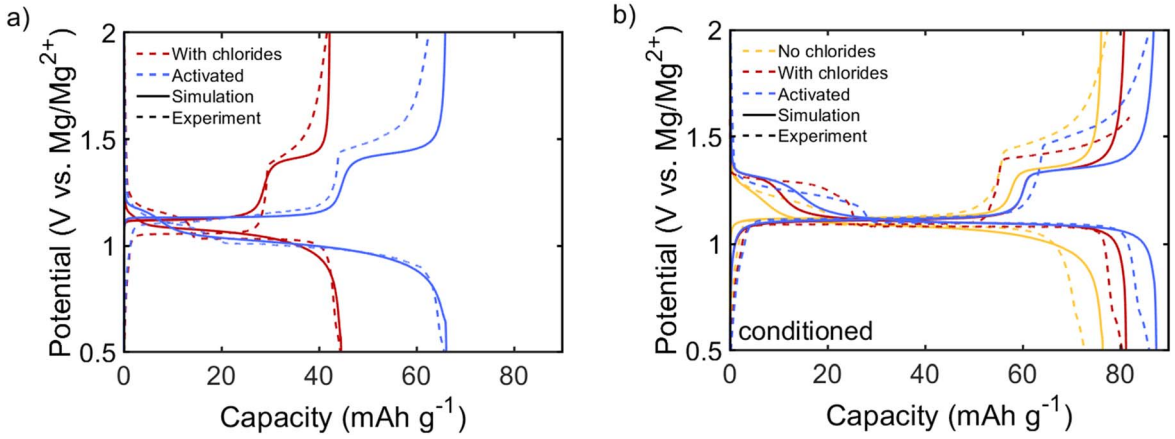

Figure 10. Second cycle charge-discharge curves of Chevrel Phase electrodes at C/10 in the different unconditioned (a) and conditioned (b) electrolyte solutions – comparison of simulated voltage profiles to experimental data (cf Fig. 9). The corresponding optimized model parameters can be found in Table IV.

contaminants block parts of the surface of the Chevrel Phase particles, considering that the CP redox potentials are lower than oxygen reduction potentials. Therefore, certain diffusion paths are not accessible, resulting in effectively longer transport pathways and, thus, smaller apparent transport parameters. Consequently, the undesired side reactions hinder the utilization and reachable capacity of the CP particles. This effective elongation of diffusion paths is not directly captured in the model but can be seen in the calculated lower solid-state diffusion constants.

Moreover, it can be seen that conditioning significantly enhances the intercalation kinetics since the reaction rate constants $k_{BV,1}$ and $k_{BV,2}$ increase about one order of magnitude by conditioning (Table IV). Therefore, the difference between the parameters of CP electrodes in the chloride containing electrolyte solutions and those of pretreated electrodes in chlorides free solutions are minor. Interestingly, the presence of chlorides does only lead to slightly higher rate constants $k_{BV,i}$ for magnesium insertion into Chevrel Phase. However, the symmetry factors related to the intercalation from the chloride-free electrolyte solutions into untreated CP cathodes are significantly smaller (Table IV). An effectively smaller $\alpha_{BV,i}$ indicates that the loss of one or more ligands of the electroactive specie is a crucial part of the electrochemical reaction pathway.[22] Consequently, the hindering effect of desolvation seems to be significantly more pronounced on the chloride-free CP surface, which can also be seen in a slopier plateau (Fig. 10). This also implies that the reaction mechanism changes due to the presence of chlorides, which support our hypothesis of a catalytic effect on the Mg ions intercalation into Chevrel Phase electrodes.

Conclusions

The presence of chloride anions has an impact on both Mg deposition-dissolution, and intercalation-deintercalation processes in $Mg[B(HFIP)_4]_2$/DME solutions. In $Mg[B(HFIP)_4]_2/MgCl_2$/DME electrolyte solutions, magnesium deposition requires much lower over-potential and occurs with higher columbic efficiency when compared to the same processes in chlorides free solutions. Despite this, adding chlorides at the right amount (0.3 M $MgCl_2$) significantly improves the over-potential for Mg deposition. But still we see a better coulombic efficiency with solutions containing 0.6 M $MgCl_2$. The macro-cycling experiments did not show any significant advantage for chlorides containing pretreated (conditioned) solutions, which contrasts with $MgTFSI_2$/DME solutions in which the presence of chlorides is mandatory for obtaining reversible Mg deposition/dissolution processes. Hence, $Mg[B(HFIP)_4]_2$/DME have intrinsic advantages. We suggest that the lack of passivation layer on the Mg electrode in $Mg[B(HFIP)_4]_2$/DME solution allows the system to run for 100 cycles, while in the $MgTFSI_2$/DME solutions, TFSI anions decomposition creates passivation layer on the Mg electrodes, that blocks the electrode and prevents the system from running more than 2 cycles.[6]

When examining the different performance of CP cathodes in unconditioned solutions with and without chlorides, we can see a much better performance in the chloride containing $Mg[B(HFIP)_4]_2/MgCl_2$/DME solutions through higher specific capacities and better kinetics, indicated by the higher current densities, and sharper peaks. However, upon using a conditioned solution, intercalation from chloride-free $Mg[B(HFIP)_4]_2$/DME is possible with a decent performance.

CP cathodes that were cycled first in chloride-containing solutions and then transferred to chloride-free solutions showed a pronounced activation effect, which enabled it to reach a similar performance to CP electrodes in chloride-containing solutions. We assume that similarly to what was found with $MgTSFI_2$/DME solutions, chlorides or Mg-Cl complexes can be strongly adsorbed on the surface of the CP active mass and catalytically enhance Mg ions intercalation.[9] We suggest that the Cl ions adsorbed to the CP surface interact with the Mg ions in solutions and facilitate their interfacial transport from solution phase into the CP active mass.

The pre-treatment of these solutions through what is termed as "conditioning" was found to play a crucial positive role in the performance of CP electrodes. Hence, the positive effect of the presence of chlorides in the conditioned solutions is much smaller than in unconditioned solutions. We suggest that unconditioned solutions are highly contaminated by active atmospheric moieties, possibly trace oxygen and water which can be reduced on CP electrodes, leading to their partial passivation, and thereby attributing to poor performance. The chlorides in these contaminated solutions may mitigate the passivation phenomena since their adsorption on the CP surface circumvents precipitation of reduced contaminants on the active mass' surface. The elimination of contaminants by conditioning therefore enables these solutions to function well as active and labile Mg ions conductor, as explained above. This is in contrast to the behavior of $MgTFSI_2$/DME, which shows that the nature of the anion plays a crucial role for enabling good performing batteries with a Cl-free electrolyte. Thereby, in contaminants free solutions, the role of chlorides on the CP electrodes performance is almost neglectable, explaining the success of the $Mg[B(HFIP)_4]_2$/DME electrolyte. Future steps to be taken are optimizing the composition and purity of these solutions, reaching cycling efficiency levels approaching 100% (as necessary for practical batteries), and testing the compatibility of $Mg[B(HFIP)_4]_2/MgCl_2$/DME and $Mg[B(HFIP)_4]_2$/DME solutions with high potential cathode materials such as V_2O_5 and sulfide coated V_2O_5 electrodes.

A further study is needed to deeply understand the effect of the presence of chlorides in these solutions, and to optimize the concentration of $MgCl_2$ in them. Further work should also address the general impact of the anions and the processes happening during

conditioning. It is also important to develop practical purification methods for $Mg[B(HFIP)_4]_2$/DME solutions or artificial interphases, which could redundant the time-consuming conditioning.

Acknowledgments

This project has received funding from the European Union's Horizon 2020 research and innovation program under grant agreement No 824066 (E-MAGIC). This work contributes to the research performed at CELEST (Center for Electrochemical Energy Storage Ulm-Karlsruhe) and was funded by the German Research Foundation (DFG) under Project ID 390874152 (POLiS Cluster of Excellence). The simulations were carried out at JUSTUS 2 cluster supported by the state of Baden-Württemberg through bwHPC and the German Research Foundation (DFG) through grant No INST 40/575–1 FUGG. A partial support for the work described herein was also obtained from the Bar-Ilan Nano-Technology Center. A partial support for the work described herein was also obtained from The Israeli Smart Transportation Research Center. A partial support for the work described herein was also obtained from the Jewish National Fund.

ORCID

Ben Dlugatch https://orcid.org/0000-0003-3921-1318
Janina Drews https://orcid.org/0000-0002-9800-6421
Ran Attias https://orcid.org/0000-0003-0528-7664
Bar Gavriel https://orcid.org/0000-0001-9970-6641
Timo Danner https://orcid.org/0000-0003-2336-6059
Arnulf Latz https://orcid.org/0000-0003-1449-8172
Doron Aurbach https://orcid.org/0000-0001-8047-9020

References

1. I. Shterenberg, M. Salama, Y. Gofer, E. Levi, and D. Aurbach, **39**, 453 (2014).
2. J. Muldoon, C. B. Bucur, and T. Gregory, *Angewandte Chemie - International Edition*, **56**, 12064 (2017).
3. D. Aurbach et al., *Nature*, **407**, 724 (2000).
4. E. Levi, M. D. Levi, O. Chasid, and D. Aurbach, *J. Electroceram.*, **22**, 13 (2009).
5. R. Mohtadi and F. Mizuno, *Beilstein J. Nanotechnol.*, **5**, 1291 (2014).
6. I. Shterenberg et al., *J. Electrochem. Soc.*, **162**, A7118 (2015).
7. M. Salama et al., *J. Phys. Chem. C*, **121**, 24909 (2017).
8. G. Bieker et al., *ACS Appl. Mater. Interfaces*, **11**, 24057 (2019).
9. Ran Attias et al., *ACS Catalysis*, **10**, 7773 (2020).
10. J. Muldoon, C. Bucur, G. W. Motors, A. G. Oliver, and J. Zajicek, *Green Energy & environment*, **4**, 345 (2013).
11. W. Zhao et al., *Chemistry - A European Journal*, **29**, 10 (2023).
12. P. Jankowski et al., *Energy Storage Mater.*, **45**, 1133 (2022).
13. B. Dlugatch et al., *ACS Appl. Mater. Interfaces*, **13**, 54894 (2021).
14. M. Kotobuki, B. Yan, and L. Lu, **54**, 227 (2023).
15. E. Levi, Y. Gofer, Y. Vestfreed, E. Lancry, and D. Aurbach, *Chem. Mater.*, **14**, 2767 (2002).
16. L. F. Wan, B. R. Perdue, C. A. Apblett, and D. Prendergast, *Chem. Mater.*, **27**, 5932 (2015).
17. C. Ling and K. Suto, *Chem. Mater.*, **29**, 3731 (2017).
18. J. Drews et al., *Batteries and Supercaps*, **6**, 1 (2023).
19. Z. Li et al., *ACS Appl. Mater. Interfaces*, **13**, 33123 (2021).
20. Z. Zhao-Karger, M. E. Gil Bardaji, O. Fuhr, and M. Fichtner, *J Mater Chem A Mater*, **5**, 10815 (2017).
21. A. Latz and J. Zausch, *J. Power Sources*, **196**, 3296 (2011).
22. J. Drews et al., *ChemSusChem*, **14**, 4820 (2021).
23. J. Drews et al., *ChemSusChem*, **13**, 3599 (2020).
24. P. T. Kissinger, W. Lafayette, and W. R. Heineman, *ACS chemical education*, **9**, 702 (1983).
25. R. Attias, B. Dlugatch, M. S. Chae, Y. Goffer, and D. Aurbach, *Electrochem. Commun.*, **124**, 3229 (2021).
26. M. Salama et al., *J. Phys. Chem. C*, **120**, 19586 (2016).
27. V. Prabhakaran et al., *ACS Appl. Mater. Interfaces*, **15**, 7518 (2023).
28. N. Sa et al., *RSC Adv.*, **6**, 113663 (2016).
29. N. N. Rajput, X. Qu, N. Sa, A. K. Burrell, and K. A. Persson, *J. Am. Chem. Soc.*, **137**, 3411 (2015).
30. J. Self et al., *J. Phys. Chem. Lett.*, **11**, 2046 (2020).
31. A. Baskin and D. Prendergast, *J. Phys. Chem. C*, **120**, 3583 (2016).
32. D. Wang et al., *Angewandte Chemie - International Edition*, **62**, 14 (2023).